Resonant plasmonic nonlinearities of the fishnet metamaterials

M. R. Shcherbakov[1], **J. Reinhold**[2], **C. Helgert**[2], **A. Chipouline**[2], **T. Pertsch**[2], **A. A. Fedyanin**[1]

[1]Faculty of Physics, Lomonosov Moscow State University
119991 Leninskie Gory 1-2, Moscow, Russia
Fax: + 7-495-9394544; email: shcherbakov@nanolab.phys.msu.ru
[2]Friedrich Schiller University Jena, Max-Wien-Platz 1, 07743 Jena, Germany

Abstract

The nonlinear-optical response of fishnet optical metamaterial is studied. Second- and third-harmonics generation with the fundamental wave exciting different types of plasmonic resonances inside the metamaterial is studied in the angular domain. Local-field-enhanced harmonic generation is found as the fundamental wavelength is tuned in the spectral vicinity of the electric surface plasmon resonances. The angular dependences of the third harmonic generation with the fundamental at the magnetic resonance reveal the characteristic maximum which could not be explained in terms of local field resonance and might be attributed to the asymmetrical structure of the fields inside the negative-index metamaterial.

1. Introduction

Recently a great effort on experimental and theoretical studies of optical negative-index metamaterials (NIMs) has been made. Numerous experimental verifications of NIMs in the optical range [1] as well as various geometries of NIMs [2, 3] were provided. Nanostructuring may lead to unusual optical properties in nonlinear optical (NLO) response [4, 5] as well. Artificially magnetic media are of special interest from the NLO point of view since the field structure of the magnetic modes are essentially nonlocal which may give rise to additional contributions into NLO processes efficiency, e.g. symmetry breaking. However, these additional sources of NLO response in magnetic resonances have not been demonstrated yet. In this paper the second- and third-harmonic generation (SHG and THG) from the fishnet NIM is studied. The results reveal different mechanisms of harmonic generation for the fundamental wavelength exciting different types of plasmonic resonances inside the structure.

2. Results

The proposed structure was defined by e-beam-lithography and lift-off technique on a SiO_2 substrate. The structure has a period of 500 nm in both lateral directions. The thicknesses of the Au films and the intermediate dielectric MgO film are 20 nm and 35 nm, respectively. Spectroscopy of the linear absorption for different angles of incidence with the angle varying from 0° to 50° was carried out. The visible absorption spectra demonstrate the band structure of the (1,0) grating SPPs coupled to the surface of the film via the first diffraction orders at the Au-SiO2 and Au-air interfaces as a series of Fano-type resonances alternating their position with the increase of the angle of incidence. The normal incidence IR absorption spectrum demonstrates an absorption peak corresponding to the excitation of the magnetic plasmon mode, which position is blue-shifted as the angle of incidence is increased.

ISBN 978-952-67611-0-7

For the nonlinear measurements in the electric resonance region we used the setup based on a tunable femtosecond pulse oscillator operating at the wavelengths of 750 nm or 800 nm. A setup based on an optical parametric amplifier was used operating at the wavelengths of 1540 nm (in the magnetic resonance of the metamaterial) and of 1600 nm (slightly out of the magnetic resonance of the metamaterial). In both setups we used the p-in, p-out polarization configuration—illuminating with p-polarized light and selecting only the p-polarized part before the detector. For all measurements spectral filtering before the sample and the detector was used for picking up the desired wavelengths.

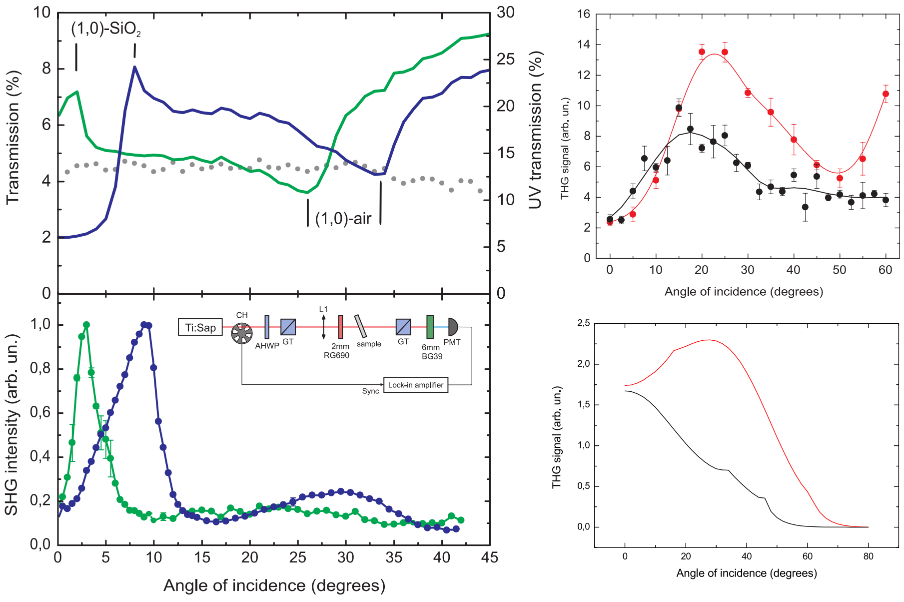

Fig. 1: Left top: linear transmission coefficient of the metamaterial as a function of the angle of incidence at the wavelengths of $\lambda = 750\,\text{nm}$ (blue curve) and $\lambda = 800\,\text{nm}$ (green curve). Grey dots demonstrate the 2ω frequency linear transmission ($\lambda = 400\,\text{nm}$). Left bottom: angular dependences of p-in, p-out SHG intensity from the fishnet metamaterial at the fundamental wavelengths of $\lambda = 750\,\text{nm}$ (blue dots) and $\lambda = 800\,\text{nm}$ (green dots). Inset shows the experimental setup. Right top: Angular dependences of the p-in, p-out THG intensity from the metamaterial at the magnetic resonance. Fundamental wavelengths are $\lambda_\omega = 1.54\,\mu\text{m}$ (in the resonance, red dots) and $\lambda_\omega = 1.60\,\mu\text{m}$ (out of the resonance, black dots). The curves are guides for the eye. Right bottom: calculated angular dependences of the p-in, p-out THG intensity from the metamaterial at the magnetic resonance. Fundamental wavelengths are of $\lambda_\omega = 1.80\,\mu\text{m}$ (in the resonance, red curve) and $\lambda_\omega = 1.90\,\mu\text{m}$ (out of the resonance, black curve).

The p-polarized incident light was used to excite the SPP modes in the metamaterial in the visible. This led to the forward SHG enhancement at particular angles corresponding to the SPP phase-matching conditions. The angular spectra shown in Fig. 1 demonstrate the 10-fold SHG enhancement in the form of sharp peaks at the angles of the resonant SPP-mediated transmission. THG was measured in the forward direction with the fundamental frequency exciting the magnetic resonance. The angular spectra of THG are provided in Fig. 1 for the fundamental frequencies wavelengths of $\lambda_\omega = 1.54\,\mu\text{m}$ and $\lambda_\omega = 1.60\,\mu\text{m}$. The shorter wavelength lies at the magnetic resonance position for normal incidence and the longer one is at the resonance for no angle of incidence. The maximum of the THG signal is seen at the angles of incidence around 20°. Forward THG signal was also simulated by means of nonlinear modification of the Fourier modal method at the magnetic resonance and outside the resonance. The calculation shows the qualitative agreement between the angular spectra. The position of the THG peak is situated at an angle of about 30° for the fundamental frequency at the magnetic resonance of the fishnet NIM.

3. Discussion

The data on the SHG with the fundamental frequency situated near the electric SPP resonances of the sample reveal the local-field-enhanced nonlinear response of the metamaterial. Indeed, the sharp angular-domain SHG peaks coincide with the peaks of SPP-mediated transmission, which could be understood in terms of the nonlinear polarization expressed as:

$$\mathbf{P}^{(n)} = \int_V \hat{L}(\mathbf{r}, n\omega) : \hat{\chi}^{(n)} : \left(\hat{L}(\mathbf{r}, \omega) : \mathbf{E}_0(\omega)\right)^n dV, \tag{1}$$

where $\mathbf{P}^{(n)}$ is the nth-order nonlinear polarization of the medium, $\hat{L}(\mathbf{r}, n\omega)$ is the local-field factor at the $n\omega$ frequency, $\hat{\chi}^{(n)}$ is the nonlinear succeptibility tensor, $\hat{L}(\mathbf{r}, \omega)$ is the factor at the fundamental frequency and $\mathbf{E}_0(\omega)$ is the fundamental wave E-field. $\hat{L}(\mathbf{r}, n\omega)$ is almost angle-independent and $\hat{\chi}^{(n)}$ components do not usually possess such strong angular dispersion. Therefore, the main contribution to the SHG at the electric resonances belongs to the local-field factor $\hat{L}(\mathbf{r}, \omega)$ which is greatly enhanced by the field of the SPPs.

Plasmon-enhanced THG at the magnetic resonance of NIMs was reported previously. It was shown that the THG spectra obey the principles of the local-field enhanced nonlinear response. However, using the approach stated by expression (1) we show that one cannot explain the angular-resolved THG data acquired at the magnetic resonance by means of local-field enhancement of the nonlinear effects. Equation (1) states that the angular dependence of the THG effect may depend on angular dependences of $\hat{L}(\mathbf{r}, 3\omega)$, $\hat{L}(\mathbf{r}, \omega)$ and/or $\hat{\chi}^{(3)}$. The former two do not explain the maximum found in the angular THG dependences. The data on the linear absorption and transmission demonstrate almost angle-invariant transmission at 3ω and monotonously decreasing plasmonic absorption at ω. If one follows the logic of the local-field-enhanced harmonic generation this data would mean the monotonic decrease of the p-in, p-out THG as a function of the angle of incidence. In contrast, we observe a distinct maximum both in experimental and FMM data. Such a behavior of the angular spectra is likely to be explained in terms of the angular dispersion of $\hat{\chi}^{(3)}$ contribution which is out of the scope of this paper.

4. Conclusion

To conclude, we have shown by means of second- and third-harmonic generation that different physical mechanisms bring up the nonlinear response of the negative index metamaterial depending on the type of resonance excited by the fundamental wave. It is shown that the nonlinear response of the metamaterial with the fundamental wavelength exciting the electric surface plasmon-polariton resonances is governed by the local field enhancement factor. On the other hand, non-monotonous angular dependences of the third-harmonic generation driven by the fundamental wavelength exciting the magnetic resonance are built by the combination of different $\hat{\chi}^{(3)}$-tensor components. The given data are expected to contribute to the understanding of the problem of the nonlinear optical response of the negative-index metamaterials.

References

[1] C. M. Soukoulis et al., Negative refractive index at optical wavelengths, *Science*, vol. 315, p. 47, 2007.

[2] V. M. Shalaev et al. Negative index of refarction in optical metamaterials, *Optics Letters*, vol. 30, p. 3356, 2005.

[3] S. Zhang et al., Experimental demonstration of near-infrared negative-index metamaterials, *Physical Review Letters*, vol. 95, p. 137404, 2005.

[4] M. W. Klein et al., Second-harmonic generation from magnetic metamaterials, *Science*, vol. 313, p. 502, 2006.

[5] I. V. Shadrivov et al., Second-harmonic generation in nonlinear left-handed metamaterials, *Journal of Optical Society of America B*, vol. 23, p. 529, 2006.